EUKARYOTIC CELL, June 2002, p. 391–400 Vol. 1, No. 3
1535-9778/02/$04.00+0 DOI: 10.1128/EC.1.3.391–400.2002

Localization, Regulation, and Substrate Transport Properties of Bpt1p, a *Saccharomyces cerevisiae* MRP-Type ABC Transporter

Kailash Gulshan Sharma,[1] Deborah L. Mason,[2] Guosheng Liu,[3] Philip A. Rea,[3] Anand K. Bachhawat,[1]* and Susan Michaelis[2]*

Department of Cell Biology, The Johns Hopkins University School of Medicine, Baltimore, Maryland 21205[2]; Institute of Microbial Technology, Chandigarh 160 036, India[1]; and Plant Science Institute, Department of Biology, University of Pennsylvania, Philadelphia, Pennsylvania 19104[3]

Received 26 December 2001/Accepted 11 March 2002

Saccharomyces cerevisiae **Bpt1p is an ATP-binding cassette (ABC) protein that belongs to the MRP subfamily and is a close homologue of the glutathione conjugate (GS conjugate) transporter Ycf1p. The function of Bpt1p has previously been evaluated only in vitro, by using nonphysiological substrates. In the present study we examined the localization, regulation, and transport properties of Bpt1p in vivo, as well as its capacity to transport a set of prototypical MRP substrates in vitro. Our results show that Bpt1p, like Ycf1p, localizes to the yeast vacuolar membrane, plays a role in cadmium detoxification and *ade2* pigmentation in vivo, and can participate in the transport of GS conjugates and glucuronate conjugates, as well as free glutathione, in vitro. However, in all of these cases the contribution of Bpt1p is substantially less than that of Ycf1p. In addition, the expression patterns of *YCF1* and *BPT1* differ significantly. Whereas *YCF1* expression is markedly increased by cadmium, adenine limitation in an *ade2* strain, or overexpression of the stress-responsive transcription factor Yap1p, *BPT1* expression is only modestly affected under these conditions. Thus, although the functional capabilities of Bpt1p and Ycf1p overlap, their differences in regulation and substrate preference imply that they contribute to cellular detoxification processes in different ways.**

With the complete genome of numerous organisms now in hand, the ATP-binding cassette (ABC) transporter superfamily has emerged as the largest membrane protein superfamily in both prokaryotes and eukaryotes, including microbes, plants, and animals (10–12, 17, 40, 45). Members of this superfamily catalyze the MgATP-energized transport of a broad range of substrates across biological membranes. Mutational loss of function of ABC proteins has been implicated in an increasing number of inherited diseases (11), and overexpression of certain ABC transporters has been shown to enhance multidrug resistance and the elimination of xenobiotics (1, 2). Consequently, elucidation of the biochemical activity, substrate specificity, and physiological regulation of ABC transporters is of both clinical and general biological significance.

Phylogenetic analysis has provided a valuable road map for formulating hypotheses about the function and substrate(s) of a particular transporter. ABC proteins can be divided into seven subfamilies based on sequence relatedness, designated ABCA through ABCG (11, 12, 45; http://nutrigene.4t.com/humanabc.htm). The emergent view is that members of a particular subfamily are likely to exhibit some degree of overlap in substrate specificity and/or function. This point is well illustrated by members of the human ABCC subfamily, also designated the multidrug resistance-associated protein (MRP) subfamily, several of which participate in cellular detoxification processes.

In humans, the ABCC/MRP subfamily contains 12 members, 5 of which (MRP1 through MRP5) are implicated in multidrug transport. Critically, most drugs are either transported by the MRPs in the form of conjugates of glutathione (GS), glucuronide, or sulfate or, alternatively, are not conjugated but instead undergo cotransport with free glutathione (GSH) (2). In addition to exogenously added drugs, molecules that are endogenously produced in cells during normal physiological processes can also be MRP substrates. For instance, inherited defects in the *MRP2* gene result in Dubin-Johnson syndrome, a disorder characterized by reduced excretion of bilirubin-glucuronides from liver cells (35, 36, 48). The general consensus is that MRPs mediate cellular detoxification processes by excreting potentially harmful endogenously and exogenously derived compounds, after these compounds have been rendered anionic by conjugation to GSH or glucuronate, or through complexing with GSH.

To gain further insight into multidrug resistance, it is important to understand how an organism may benefit by having multiple, highly homologous MRPs. Comparisons of the properties of the human MRP1, MRP2, and MRP3 transporters suggest several possibilities (3, 18, 21). First, these three MRPs appear to have overlapping, but distinct, substrate and kinetic profiles. Second, their intracellular sites of localization differ. Third, their regulatory properties differ, resulting in distinct patterns of tissue expression and/or response to extracellular stress (i.e., oxidative stress) (7). The combined effect of differences in these three parameters (spectrum of substrate specificity, location, and regulation) could impart a sufficiently high degree of specificity and flexibility to explain the distinctive

* Corresponding author. Mailing address for Susan Michaelis: Department of Cell Biology, The Johns Hopkins University School of Medicine, 725 North Wolfe St., Baltimore, MD 21205-2196. Phone: (410) 955-7274. Fax: (410) 955-4129. E-mail: michaelis@jhmi.edu. Mailing address for Anand K. Bachhawat: Institute of Microbial Technology, Chandigarh 160 036, India. Phone: 91-172-690-908. Fax: 91-172-690-632. E-mail: abachhawat@hotmail.com.

TABLE 1. Strains used in this study

Strain	Relevant genotype	Reference or source
ABC154[a]	*MAT***a** *ura3-52 leu2-Δ1 lys2-801 his3Δ200 trp1Δ63 ade2-101*	42
ABC470	*MAT***a** *ycf1Δ::KanMX2 ura3-52 leu2-Δ1 lys2-801 his3Δ200 trp1Δ63 ade2-101*	5
ABC791	*MAT***a** *bpt1Δ::KanMX2 ura3-52 leu2-Δ1 lys2-801 his 3Δ200 trp1Δ63 ade2-101*	This study
ABC794	*MATα ycf1Δ::KanMX2 bpt1Δ::KanMX2 ura3-52 leu2-Δ1 lys2-801 his 3Δ200 trp1Δ63 ade2-101*	This study
SEY6210	*MATα leu2-3,112 ura3-52 his3-Δ200 trp1-Δ901 lys2-801 suc2-Δ9 Mel*$^-$	8
SM13	*MATα leu2-3,112 ura3-52 his3-Δ200 trp1-Δ901 lys2-801 suc2-Δ9 Mel*$^-$ *yap1-2::hisG*	8
SM1058	*MAT***a** *trp1 leu2 ura3 his4 can1*	30
SM3794	*MAT***a** *bpt1Δ::KanMX4 trp1 leu2 ura3 his4 can1*	This study
SM3851	*MAT***a** *ycf1Δ trp1 leu2 ura3 his4 can1*	This study
SM3858	*MAT***a** *bpt1Δ::KanMX4 ycf1Δ trp1 leu2 ura3 his4 can1*	This study
SM4643	*MAT***a** *YCF1-GFP trp1 leu2 ura3 his4 can1*	This study
SM4787	*MAT***a** *bpt1Δ::KanMX4::BPT1-GFP URA3 trp1 leu2 ura3 his4 can1*	This study

[a] This strain is designated YPH499 elsewhere (42).

physiological roles of particular MRPs and to account for their large numbers in all organisms.

The yeast *Saccharomyces cerevisiae* presents a highly manipulable system for the genetic and biochemical analysis of both endogenous and heterologous ABC proteins (12, 45). Yeast encodes six MRP subfamily members, of which the vacuolar GS conjugate pump Ycf1p is the most thoroughly characterized (23, 25). Ycf1p can transport organic GS conjugates and Cd · glutathione (Cd · GS) complexes into the vacuole (23, 25, 44). Deletion of *YCF1* results in hypersensitivity to cadmium, while overexpression confers cadmium resistance. Ycf1p shares many biochemical properties with mammalian MRP1, and significantly, human MRP1 restores GS conjugate transport and cadmium resistance in *ycf1*-defective yeast strains (46). In addition, Ycf1p has been found to confer resistance to arsenite and diamide, and it is required for the vacuolar accumulation of a pigment precursor in *ade2* mutants (5, 14, 49).

The closest homologue of *YCF1* in yeast is *YLL015*. Since *YLL015* was discovered through the yeast genome sequence project and not from mutant or overexpression screens, its in vivo function as a transporter has been only hypothetical. Recently, a biochemical study indicated that *YLL015*, like *YCF1*, can mediate the in vitro transport of unconjugated bilirubin into yeast vacuole-derived vesicles (37). Accordingly, the gene has been designated *BPT1* (named *BPT* for bile pigment transporter), even though this particular substrate is unlikely to have direct physiological relevance for yeast. Bpt1p and Ycf1p have also been shown to have overlapping activity for the in vitro transport of other nonphysiological substrates, including several Gd-based magnetic resonance imaging (MRI) contrast agents (34).

In the present study we have compared the localization, regulation, and transport properties of Bpt1p and Ycflp both in vivo and in vitro. Our results show that Bpt1p, like Ycf1p, localizes to the vacuolar membrane, participates in cadmium detoxification and *ade2* pigmentation in vivo, and has the capacity to catalyze the transport of GS and glucuronate conjugates, as well as that of free GSH in vitro. Although the transport properties of Bpt1p and Ycf1p overlap, their cellular impacts seem to differ considerably: the overall phenotypic and biochemical contributions of *YCF1* consistently exceed those of *BPT1*. These differences in contribution may be due in part to differences in substrate selectivity and in part to the relative levels of each transporter, as determined by differences in their patterns of regulation. An interesting feature observed for some of the substrates was an unexpected dependence of Bpt1p on Ycf1p for maximal transport activity in vitro. Of the several potential explanations for this phenomenon, one intriguing possibility is that Bpt1p and Ycf1p form functional heterodimers.

MATERIALS AND METHODS

Yeast strains. The strains used in this study are listed in Table 1. A chromosomal disruption of *BPT1* was generated in the *ade2* haploid strains YPH499 (here designated ABC154) and YPH500 (42) by using PCR-mediated gene disruption with the *KanMX2* module (47) to replace codons 428 to 736 of Bpt1p, yielding ABC791 and ABC790, respectively. A double mutant, ABC794 (*ycf1Δ::KanMX2 bpt1Δ::KanMX2*), was constructed by dissecting tetrads derived from a diploid generated by a cross between ABC470 and ABC790. Double-disruption segregants were found to be viable. The presence of both disruptions was confirmed by PCR.

Single and double disruptions of *YCF1* and *BPT1* in the *ADE2* diploid strain SM1060 (30) were also generated. Chromosomal *YCF1* was disrupted from codon 1 to 1439 by the standard two-step integration-excision method using plasmid pJAW53, as previously described (50). The diploid was sporulated and the tetrads were dissected to obtain both *MAT***a** (SM3851) and *MATα* (SM3852) *ycf1* disruptants. A precise open reading frame (ORF) deletion allele of *BPT1* was generated in SM1060 by PCR-mediated gene disruption with the *KanMX4* module (4, 47). The diploid was sporulated and the tetrads were dissected to obtain both *MAT***a** (SM3794) and *MATα* (SM3795) *bpt1* disruptants. The double mutant SM3858 (*bpt1Δ::KanMX4 ycf1Δ*) was constructed by dissecting tetrads derived from a diploid generated by a cross between SM3852 and SM3794. The disruptions were confirmed by Southern blot analysis.

A strain containing chromosomal *BPT1-GFP* was generated by transforming *Swa*I-digested pSM1849 into strain SM3794 (*bpt1Δ*) and selecting for Ura$^+$ transformants. One of the transformants, SM4787, which contains *BPT1-GFP* integrated adjacent to the *KanMX4*-disrupted copy of *BPT1*, was confirmed for Bpt1p-green fluorescent protein (GFP) expression by Western blot analysis. A strain containing chromosomal *YCF1-GFP* was generated by the standard two step integration-excision method by transforming *Avr*II-digested pSM1817 into strain SM3851 (*ycf1Δ*) and selecting for Ura$^+$ transformants. The resulting strain, SM4643, contains *YCF1-GFP* at the *YCF1* locus. Correct integration of *YCF1-GFP* was confirmed by Southern blot analysis, and the presence of Ycf1p-GFP was confirmed by Western blot analysis.

Plasmids and their construction. Plasmids used in this study are listed in Table 2. Plasmid pSM1487 (*CEN URA3 BPT1*) contains the complete *BPT1* ORF flanked by its native 5′ upstream and 3′ downstream regions (515 and 500 bp, respectively) and was constructed in two steps. First, the 5′ upstream and 3′ downstream regions of *BPT1* were amplified from the genome by PCR and subcloned by three-way ligation into pRS316 (*CEN URA3*) (42). Next, the *BPT1* ORF was cloned into this vector by levitating it from the genome (32). The *BPT1* coding sequence in the resulting plasmid, pSM1487 (*CEN URA3 BPT1*), was confirmed by DNA sequence analysis. The multicopy plasmid pSM1488 (2μm *URA3 BPT1*) contains a 5.7-kb *Kpn*I-*Not*I fragment from pSM1487 subcloned into the same sites of pSM217 (2μm *URA3*) (6). A GFP-tagged version of *BPT1* was constructed by fusing the GFP coding sequence (F64L S65T) immediately before the stop codon of *BPT1* by PCR-mediated recombinational cloning (32)

TABLE 2. Plasmids used in this study

Plasmid	Relevant genotype[a]	Reference or source
pAB851	2μm *URA3* P_{BPT1}-*lacZ*	This study
pAB852	2μm *URA3* P_{YCF1}-*lacZ*	This study
pJAW53	YIp 5′-1,018 nt-*YCF1-hisG-URA3-hisG*-3′-1,356 nt-*YCF1*	50
pSM217	2μm *URA3*	6
pSM1490	2μm *URA3 BPT1-GFP*	This study
pSM1753	2μm *URA3 YCF1-GFP*	This study
pSM1817	YIp *URA3 YCF1-GFP*	This study
pSM1849	YIp *URA3 BPT1-GFP*	This study
YEp351-*YAP1*	2μm *LEU2 YAP1*	50

[a] YIp denotes a yeast integrating plasmid; nt, nucleotides.

to create pSM1489 (*CEN URA3 BPT1-GFP*). To generate a multicopy version of this construct, a 6.5-kb *Kpn*I-*Not*I fragment from pSM1489 was subcloned into the same sites of pSM217, generating pSM1490 (2μm *URA3 BPT1-GFP*). A GFP-tagged version of *YCF1* was generated by subcloning a 6.0-kb *Kpn*I-*Sac*I fragment from pJAW50 (50) into *Kpn*I-*Sac*I-digested pSM217. Next, the coding sequence for GFP (pQBI25; Quantum Biotechnologies, Inc., Montreal, Quebec, Canada) was fused immediately before the stop codon of *YCF1* by PCR-mediated recombinational cloning (32) to yield pSM1753 (2μm *URA3 YCF1-GFP*).

To generate an integrating plasmid expressing *BPT1-GFP*, we constructed pSM1849 by subcloning an 8.2-kb *Pvu*I fragment from pSM1490 into the same sites of pRS306 (42). The *YCF1-GFP* integrating plasmid pSM1817 contains the coding sequence from pSM1753 and 1,092 bases of the region downstream of the *YCF1* ORF amplified from pJAW53 (50) subcloned into pRS306 (42).

To construct the *BPT1* promoter-reporter fusion plasmid pAB851 (2μm *URA3* P_{BPT1}-*lacZ*), a purified PCR product containing 448 bases upstream of the *BPT1* ORF was subcloned into the *Sma*I site of pBluescript (Stratagene, La Jolla, Calif.). Next, an *Xho*I-*Bam*HI fragment was excised and cloned into the *Bam*HI-*Xho*I sites of pLG699-Z (2μm *URA3 lacZ*) (16), yielding pAB851. The *YCF1* promoter-reporter fusion plasmid pAB852 (2μm *URA3* P_{YCF1}-*lacZ*) was constructed by amplifying 418 bases upstream of the *YCF1* ORF and subcloning this purified PCR product into the *Xho*I-*Bam*HI sites of pLG699-Z. The *YCF1* promoter differed from the published sequence at position −302, containing an insertion of C at this position. The same insertion was observed in clones from completely independent and separate PCRs and is therefore not an artifact of PCR. The primers for both plasmids were designed to enable in-frame fusions with the *lacZ* gene at the *Bam*HI site in pLG699-Z. The sequences of the resultant in-frame fusions were confirmed by sequencing.

The sequences of oligonucleotides used for the strain and plasmid constructions will be furnished upon request.

Media and growth conditions. Cells were routinely grown at 30°C in complete (yeast extract-peptone-dextrose [YPD]) medium or minimal drop-out medium (i.e., synthetic complete medium without Ura [SC-Ura]) as previously described (30). YPD medium containing different concentrations of $CdCl_2$ was prepared by addition of the required amount of $CdCl_2$ immediately prior to the growth experiment. For pigment quantitation, the liquid YPD medium was limiting for adenine and contained 0.5% yeast extract rather than 1% yeast extract. The minimal drop-out plates used for the pigmentation test in Fig. 2 contained a limited amount of adenine (7.5 mg per liter). The plates used for the cadmium spot test were prepared by adding the indicated concentration of $CdSO_4$ to the minimal plate medium.

Fluorescence microscopy. Log-phase cells expressing GFP-tagged Bpt1p and GFP-tagged Ycf1p were examined at ×100 magnification on a polylysine-coated slide by using a Zeiss Axioskop 2 microscope equipped with fluorescence (HQ Endow GFP) and Nomarski optics (Zeiss, Thornwood, N.Y.). Images were captured with a Cooke charge-coupled device camera and IP Lab Spectrum software (Biovision Technologies, Inc., Exton, Pa.).

β-Galactosidase reporter assays. *S. cerevisiae* SEY6210 (wild type [WT]) or SM13 (*yap1*-Δ*2*) cells were singly transformed with the β-galactosidase reporter plasmids pAB851 (P_{BPT1}-*lacZ*) and pAB852 (P_{YCF1}-*lacZ*) or doubly transformed with one of these reporter plasmids and YEp351-*YAP1* (50), which overproduces Yap1p. The WT strain ABC154 (*ade2*) was also singly transformed with the reporter plasmids to compare the transcriptional regulation of *YCF1* and *BPT1* in the presence of $CdCl_2$ or a limited amount of adenine. Transformants were grown to log phase in selective medium, harvested, washed, resuspended in Z buffer, and assayed for β-galactosidase activity (38). Measurements were carried out in triplicate, and activity was expressed as β-galactosidase units per OD_{600} (optical density at 600 nm) unit of cells.

Quantitation of the red pigment that accumulates in an *ade2* strain. To quantitate the extent of pigment formation during growth of *ade2* strains on adenine-limiting medium, cells were grown to an OD_{600} ranging between 2.9 and 3.2 in YPD medium containing 0.5% yeast extract. An equal number of cells from each strain (as determined by OD_{600}) was harvested and washed with sterile water. Cells were lysed in 5% sulfosalicylic acid by using glass beads, and cell debris was removed by centrifugation at 15 K for 5 min. The amount of the pigment was estimated by recording the absorbance at 530 nm (λ_{max}). Control extracts were prepared in a similar manner by using strain ABC591 (*gsh1*Δ) (41) grown in the presence of excess adenine (5).

Growth inhibition by cadmium. To examine growth in liquid medium, cells grown to saturation in YPD medium were subcultured at a starting OD_{600} of ~0.1 into YPD medium containing different concentrations of $CdCl_2$ and the extent of growth after 30 h was determined by measuring the OD_{600}. The growth rate of each culture was also determined by taking OD_{600} readings at multiple intervals throughout the entire 30-h period. In all cases, an alteration in the extent of growth after 30 h is reflected as a corresponding alteration in the rate of growth (data not shown).

To examine growth on plates, cells were grown overnight to saturation in minimal medium, then subcultured at a 1:500 dilution into the same medium, and grown overnight at 30°C to an OD_{600} of approximately 1.0. This overnight culture was diluted to an OD_{600} of 0.1, which in turn was diluted in 10-fold increments. Five microliters of each 10-fold dilution was spotted onto SC-Ura plates containing different concentrations of $CdSO_4$ and incubated for 3 days at 30°C.

Transport substrates. Radiolabeled 2,4-dinitrophenyl-glutathione ([^{3}H]DNP-GS) (418.7 mCi/mmol) was synthesized and purified as described previously (24). Radiolabeled GSH ([^{3}H]GSH) (44 Ci/mmol) and β-estradiol 17-(β-D-glucuronide) ([^{3}H]$E_2$17βG) (55 mCi/mmol) were purchased from DuPont, NEN.

Transport assays. For in vitro transport measurements, vacuoles were isolated by the Ficoll floatation technique from cells grown in YPD medium and were vesiculated as described previously (23). The uptake of [^{3}H]DNP-GS, [^{3}H]$E_2$17βG, or [^{3}H]GSH by yeast vacuolar membrane vesicles was measured at 25°C in 200-μl volumes containing 3 mM ATP, 3 mM $MgSO_4$, 5 μM gramicidin-D, 10 mM creatine phosphate, 16 U of creatine phosphate kinase/ml, 50 mM KCl, 1 mg of bovine serum albumin/ml, 400 mM sorbitol, 25 mM Tris-morpholineethanesulfonic acid (MES) buffer (pH 8.0), and the indicated concentrations of radiolabeled transport substrate. In the case of [^{3}H]GSH, oxidation and the formation of oxidized GSH, [^{3}H]GSSG, was minimized by degassing all solutions before the dissolution of GSH and by purging the freshly prepared GSH stock solutions and uptake media with nitrogen gas immediately before use. In all cases, uptake was initiated by the addition of membrane vesicles and was terminated by addition of 1 ml of ice-cold wash medium (400 mM sorbitol in 3 mM Tris-MES buffer [pH 8.0]) and vacuum filtration of the suspension through prewetted Millipore Durapore (GVWP) filters (pore size, 0.22 μm). Filters were rinsed twice with wash medium, and the radioactivity retained was determined by liquid scintillation counting. Nonenergized (MgATP-independent) uptake was estimated by the same procedure, except that ATP was omitted from the uptake medium.

Computations. Lines of best fit and kinetic parameters were estimated by nonlinear least-squares analysis (29) using the Ultrafit nonlinear least-squares curve-fitting package from BioSoft (Ferguson, Mo.).

RESULTS

Bpt1p, a homologue of yeast Ycf1p and mammalian MRP1, localizes to the yeast vacuolar membrane. The GS conjugate transport activities of Ycf1p in vivo and in vitro are well es-

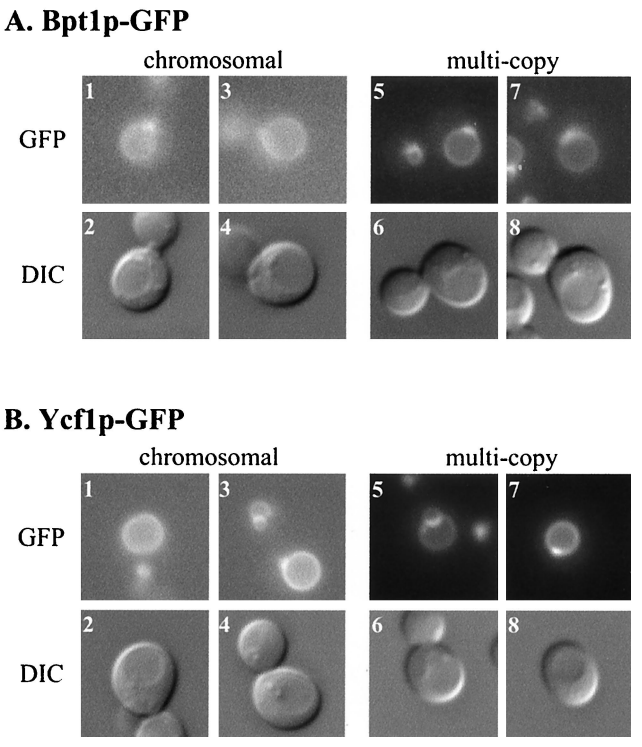

FIG. 1. Bpt1p, like Ycf1p, localizes to the vacuolar membrane. The GFP fluorescence pattern of cells expressing Bpt1p-GFP (A) or Ycf1p-GFP (B) from the chromosome (panels 1 and 3) or from a multicopy plasmid (panels 5 and 7) is shown. In the corresponding Nomarski (DIC) images of these cells (A and B, panels 2, 4, 6, and 8), the vacuole appears as an indentation. Strains used are SM4787 (A, panels 1 to 4), SM3794/pSM1490 (A, panels 5 to 8), SM4643 (B, panels 1 to 4), and SM3851/pSM1753 (B, panels 5 to 8).

tablished (23, 25). In this study we analyzed Bpt1p, the closest yeast homologue of Ycf1p. Bpt1p shares strong overall homology with Ycf1p (42% identity and 59% similarity) as well as with human MRP1 (38% identity and 57% similarity) (9). It possesses a domain organization typical of most members of the MRP subclass of ABC transporters, consisting of two membrane-spanning domains (MSDs), each with six spans, and two nucleotide binding domains (NBDs). Notably, Bpt1p and Ycf1p also contain the N-terminal extension that is the hallmark of a subset of the MRP subfamily members and consists of an additional membrane-spanning domain (MSD0) with five spans, followed by a linker (L0) region (3).

Ycf1p localizes to the vacuolar membrane, as shown by immunofluorescence and subcellular fractionation (23, 49). To localize Bpt1p, we generated a Bpt1p-GFP fusion construct, as well as its Ycf1p-GFP counterpart. The latter is fully functional, as measured by its ability to confer cadmium resistance on a *ycf1*Δ strain (data not shown). Fluorescence and Nomarski microscopy were carried out for Bpt1p-GFP and Ycf1p-GFP expressed from either the chromosome or a multicopy plasmid. Bpt1p-GFP (Fig. 1A), like Ycf1p-GFP (Fig. 1B), exhibits a clear-cut vacuolar membrane localization, as can be seen by the correspondence of the vacuole indentation observed by differential interference contrast (DIC) and GFP fluorescence patterns. The brighter areas of fluorescence appear to correspond to regions where the multiple vacuolar lobes intersect. The grainy fluorescence pattern in cells expressing single-copy versus multicopy Bpt1p-GFP and Ycf1p-GFP is due to the long exposure required to enhance the dim signal for the former. Based on the results above, Bpt1p, like Ycf1p, would therefore be expected to be an ABC transporter that delivers its cargo into the vacuole lumen.

Bpt1p contributes to the transport of the GS-conjugated compound responsible for the red pigmentation of an *ade2* strain in vivo. Since Bpt1p and Ycf1p reside in the same membrane and share significant sequence identity, we were interested to determine if they have overlapping transport functions. As a starting point for these analyses, we generated a *bpt1* null mutant by homologous gene replacement using the *KanMX2* cassette to disrupt the *BPT1* ORF in both *MAT***a** and *MAT*α haploid strains. Growth of the *bpt1* null mutant is indistinguishable from that of the isogenic WT strain (data not shown), indicating that *BPT1* is not an essential gene under normal growth conditions. Likewise, the growth of a double null mutant (*ycf1*Δ *bpt1*Δ) generated by a cross between the single mutants is similar to that of the WT, although occasionally a slight growth impairment could be observed with this strain (for example, see Table 3, growth in 0 μM $CdCl_2$).

YCF1 has been shown to play an important role in the red pigmentation of adenine biosynthetic mutants in *S. cerevisiae* (5). Specifically, strains carrying *ade1* or *ade2* mutations accumulate an intense red pigment in their vacuoles when they are grown under conditions of adenine limitation. The formation of this pigment involves a series of steps, including conjugation of GSH to the adenine biosynthetic intermediate phosphoribosylaminoimidazole (AIR), transport of AIR-GS conjugates into the vacuole in a Ycf1p-dependent manner, and further metabolism of the pigment precursor after its vacuolar sequestration. In a *ycf1* null mutant, pigmentation of an *ade2* mutant is diminished but not completely eliminated (5). Presumably, residual pigmentation occurs because another cellular transporter(s) can mediate the transport of AIR-GS conjugates.

To examine whether the residual pigmentation of the *ade2* *ycf1*Δ strain involves Bpt1p, we quantitated the extent of pigment formation in strains that had single and double disruptions of *BPT1* and *YCF1*. Quantitation was performed as described in Materials and Methods, and data are averages of four experiments ± standard deviations. Pigment accumulation, expressed as a percentage of that in the WT strain ABC154, was 96% ± 8.4% for strain ABC791 (*bpt1*Δ), 31% ± 4.3% for strain ABC470 (*ycf1*Δ), and 15% ± 6.8% for strain ABC794 (*bpt1*Δ *ycf1*Δ). Thus, as expected, pigment accumulation was substantially decreased in the *ycf1*Δ mutant (to 31% of the WT level). Notably, the deletion of *bpt1* in a *ycf1*Δ strain background resulted in a further decrease in pigmentation (to 15% of the WT level in the *ycf1*Δ *bpt1*Δ double mutant), clearly implicating Bpt1p in vacuolar pigment sequestration. However, the accumulation of pigment in the *bpt1* null mutant was not significantly different from that in the WT strain (96 versus 100%, respectively), presumably because the contribution of Ycf1p overwhelmed that of Bpt1p. Thus, while Bpt1p is not a major player in *ade2* pigmentation when Ycf1p is present, it does indeed appear to contribute to this process, as evidenced by the finding that when the Ycf1p transporter is absent, a role for Bpt1p is clearly revealed. From a genetic standpoint, the

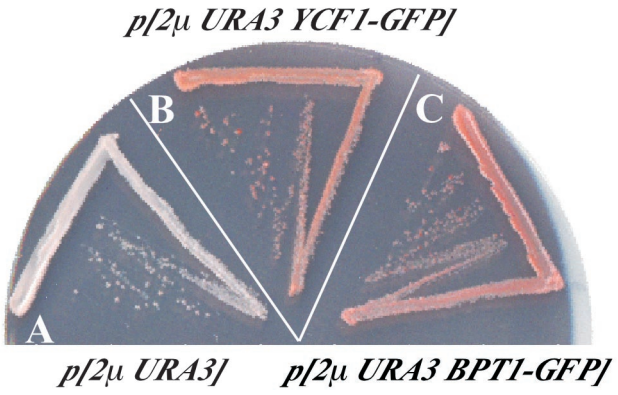

FIG. 2. The *ade2* pigmentation-defective phenotype of a double-mutant strain (*ycf1*Δ *bpt1*Δ) is complemented by a multicopy *BPT1* plasmid. Strains were streaked onto an SC-Ura plate containing limiting adenine (7.5 mg/liter) and were incubated for 3 days at 30°C. The *ycf1*Δ *bpt1*Δ double-mutant strain containing an empty vector (A) shows diminished pigmentation and is light pink. Expression of *YCF1-GFP* (B) or *BPT1-GFP* (C) from a multicopy plasmid, pSM1753 or pSM1490, respectively, complements the pigmentation defect of the *ycf1*Δ *bpt1*Δ double mutant, resulting in formation of dark-pink colonies.

*ycf1*Δ and *bpt1*Δ mutants exhibit "synthetic enhancement" of the *ade2* phenotype (15); the phenotype of the double mutant is markedly more severe than that of either of the single mutants.

The results of plate tests of the capacity of the *BPT1* gene expressed from a multicopy plasmid to restore *ade2* pigmentation in the *ycf1*Δ *bpt1*Δ double mutant are consistent with these conclusions. Whereas the *ycf1*Δ *bpt1*Δ strain containing an empty vector formed white to pale-pink colonies (Fig. 2A), the *ycf1*Δ *bpt1*Δ strain harboring a *BPT1* plasmid formed dark-pink colonies (Fig. 2C), with a pigmentation intensity comparable to that of the double-mutant strain harboring a *YCF1* plasmid (Fig. 2B). Importantly, although this result is not quantitative, it suggests that Bpt1p on its own, like Ycf1p, has the capacity to function as a transporter for the GS-conjugated *ade2* pigment precursor.

Bpt1p contributes to cadmium detoxification, as evidenced by synthetic enhancement of cadmium sensitivity in a *ycf1*Δ *bpt1*Δ double mutant. Ycfp1p contributes to cadmium detoxification in yeast by mediating the transport of Cd·GS complexes into the vacuole (25). Compared to an isogenic WT (*YCF1*) strain, a *ycf1*Δ mutant is hypersensitive to cadmium salts (44). To determine whether Bpt1p also plays a role in cadmium detoxification, we compared the growth of a WT strain with that of strains that had single and double disruptions of *BPT1* and *YCF1*, both in liquid media and on plates containing different concentrations of cadmium.

For liquid growth experiments, saturated overnight cultures of each strain were subcultured into YPD medium containing 0, 50, or 100 μM $CdCl_2$ and were propagated for 30 h. The extent of growth was determined by measuring the OD_{600} after 30 h (Table 3). All of the strains, including the WT, are subject to growth retardation by 50 or 100 μM $CdCl_2$. As reported previously, growth of the *ycf1*Δ strain was markedly retarded, here attaining only 55 and 36% of the OD_{600} of the WT at 50 and 100 μM $CdCl_2$, respectively, confirming that Ycf1p is important for cadmium resistance. In contrast, growth of the *bpt1*Δ strain was unaffected; this mutant strain attained 100% of the OD_{600} of the WT at 50 and 100 μM $CdCl_2$, indicating that Bpt1p is dispensable for cadmium detoxification when Ycf1p is functional. However, a discernible contribution of Bpt1p to cadmium detoxification was revealed in the double (*ycf1*Δ *bpt1*Δ) mutant, whose growth was significantly diminished in $CdCl_2$ relative to that of the *ycf1*Δ single mutant (36% versus 55% in 50 μM $CdCl_2$ and 21% versus 36% in 100 μM $CdCl_2$). Augmentation of the *ycf1*Δ cadmium-sensitive phenotype through the abolition of Bpt1p function is consistent with a synthetic enhancement, similar to that observed for the $Ade2^-$ phenotype. Bpt1p can contribute to cadmium detoxification in yeast, presumably by mediating the transport of Cd · GS complexes into the vacuole, albeit at modest levels compared to that of Ycf1p.

TABLE 3. Effects of cadmium on growth of WT and mutant strains

Strain[a]	OD_{600}[b] (% of WT) at:		
	0 μM $CdCl_2$	50 μM $CdCl_2$	100 μM $CdCl_2$
WT	8.4 (100)	1.1 (100)	1.1 (100)
*bpt1*Δ	8.3 (99)	1.1 (100)	1.1 (100)
*ycf1*Δ	7.9 (94)	0.6 (55)	0.4 (36)
*ycf1*Δ *bpt1*Δ	7.6 (90)	0.4 (36)	0.2 (21)

[a] Strains used were ABC154 (WT), ABC791 (*bpt1*Δ), ABC470 (*ycf1*Δ), and ABC794 (*ycf1*Δ*bpt1*Δ).

[b] Measured after 30 h of growth at 30°C. The OD_{600}s of the starting cultures were 0.14 for the WT and *bpt1*Δ strains and 0.13 for the *ycf1*Δ and *ycf1*Δ *bpt1*Δ strains.

The results of plate tests yielded the same basic conclusion, regardless of the background strain in which the single and double mutants were generated. Results with strains derived from YPH499 (42) (here designated ABC154) and EG123 (43)

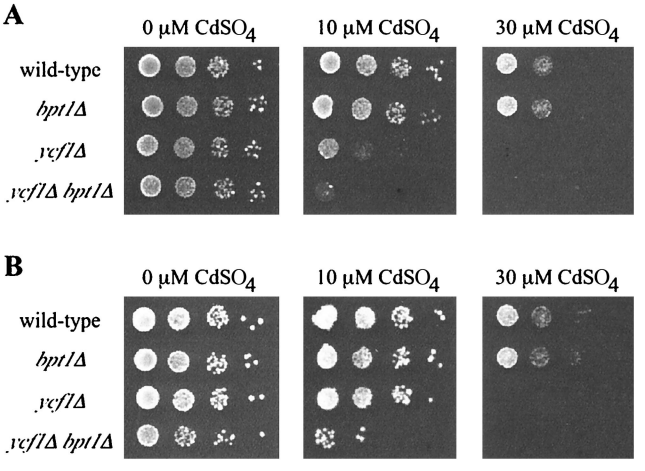

FIG. 3. Bpt1p contributes to cadmium detoxification. Strains derived from ABC154 (A) and SM1058 (B) were tested for their capacity to tolerate $CdSO_4$. An aliquot of cells at 0.1 OD, and serial 10-fold dilutions thereof, were spotted onto plates containing 0, 10, or 30 μM $CdSO_4$ and incubated at 30°C for 3 days. The strains tested all harbor the insertless plasmid pSM217 to permit growth on SC-Ura drop-out media; they are (A) ABC154 (wild-type), ABC791 (*bpt1*Δ), ABC470 (*ycf1*Δ), and ABC794 (*ycf1*Δ *bpt1*Δ); and (B) SM1058 (wild-type), SM3794 (*bpt1*Δ), SM3851 (*ycf1*Δ), and SM3858 (*ycf1*Δ *bpt1*Δ).

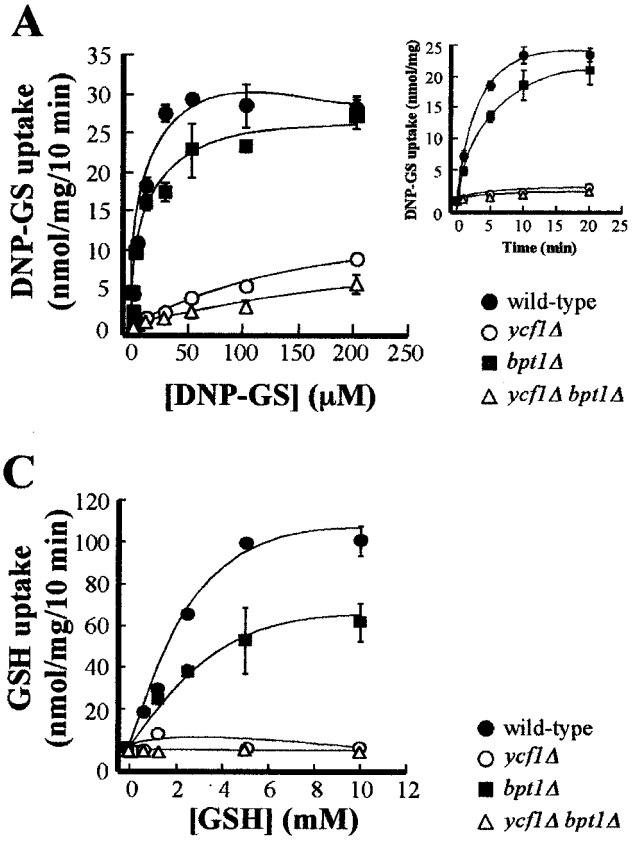

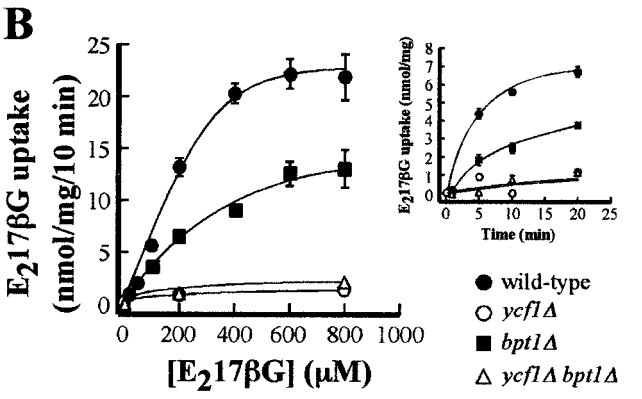

FIG. 4. MgATP-dependent uptake of [^{3}H]DNP-GS, [^{3}H]$E_2$17βG, and [^{3}H]GSH by vacuolar membrane vesicles from WT and mutant strains. For the large graphs in panels A, B, and C, MgATP-dependent uptake of the indicated transport substrates was measured for 10 min, at the concentrations of substrate indicated, in the presence or absence of 3 mM ATP. The level of uptake at each substrate concentration was calculated by subtracting the amount of radioactivity detected in the absence of ATP from that detected when ATP was present. The data were fitted to the Michaelis-Menten equation by nonlinear least-squares analysis. The values obtained for each substrate and each strain are as follows. (A) For the WT, $K_{m(\text{DNP-GS})} = 5.8 \pm 2.3$ μM and $V_{\max(\text{DNP-GS})} = 30.7 \pm 2.3$ nmol/mg/10 min; for the *bpt1*Δ strain, $K_{m(\text{DNP-GS})} = 6.3 \pm 3.8$ μM and $V_{\max(\text{DNP-GS})} = 25.3 \pm 3.0$ nmol/mg/10 min; for the *ycf1*Δ strain, $K_{m(\text{DNP-GS})} = 268.4 \pm 157$ μM and $V_{\max(\text{DNP-GS})} = 20.3 \pm 7.8$ nmol/mg/10 min. (B) For the WT, $K_{m(\text{E217βG})} = 386.0 \pm 33.0$ μM and $V_{\max(\text{E217βG})} = 35.3 \pm 13.5$ nmol/mg/10 min; for the *bpt1*Δ strain, $K_{m(\text{E217βG})} = 580.0 \pm 38.0$ μM and $V_{\max(\text{E217βG})} = 23.2 \pm 8.0$ nmol/mg/10 min. (C) For the WT, $K_{m(\text{GSH})} = 3.8 \pm 0.4$ mM and $V_{\max(\text{GSH})} = 149.4 \pm 76.3$ nmol/mg/10 min; for the *bpt1*Δ strain, $K_{m(\text{GSH})} = 3.8 \pm 0.4$ mM and $V_{\max(\text{GSH})} = 87.5 \pm 43.3$ nmol/mg/10 min. Kinetic parameters were not calculated for DNP-GS uptake by the *ycf1*Δ *bpt1*Δ strain or for $E_2$17βG and GSH uptake by the *ycf1*Δ and *ycf1*Δ *bpt1*Δ mutants, because the data did not approximate the Michaelis-Menten equation. Individual data points are means ± standard errors ($n = 3$ to 6). The insets in panels A and B show the time courses for DNP-GS and $E_2$17βG uptake, respectively. The strains used for the preparation of vacuolar vesicles are ABC154 (wild type), ABC470 (*ycf1*Δ), ABC791 (*bpt1*Δ), and ABC794 (*ycf1*Δ *bpt1*Δ).

(here designated SM1058) are shown in Fig. 3A and B, respectively. A culture of each strain was diluted to an OD_{600} of 0.1, and serial dilutions were spotted onto plates without (0 μM) and with (10 and 30 μM) cadmium. In the absence of cadmium, the growth of all strains is essentially equivalent (Fig. 3, 0 μM $CdSO_4$). On a plate containing the small amount of cadmium (10 μM $CdSO_4$), growth of the *bpt1*Δ single mutant in the ABC154 strain background is equivalent to that of the WT strain. However, a role for Bpt1p is clearly revealed in the double mutant *ycf1*Δ *bpt1*Δ at this cadmium concentration (Fig. 3A; compare the modest growth of the *ycf1*Δ strain to the lack of growth of the *ycf1*Δ *bpt1*Δ double-mutant strain at 10 μM $CdSO_4$). Although the phenotype of the SM1058-derived strains on 10 μM cadmium is not as severe as that of the ABC154-derived strains (compare the growth of the *ycf1*Δ strain for each), a role for Bpt1p is also revealed by the double mutant *ycf1*Δ *bpt1*Δ in this strain background on 10 μM $CdSO_4$ (Fig. 3B). On plates containing the higher concentration (30 μM $CdSO_4$), cadmium toxicity is of sufficient severity that neither the *ycf1*Δ single mutant nor the *ycf1*Δ *bpt1*Δ double mutant grows.

Bpt1p plays a role in the in vitro transport of GS conjugates, glucuronides, and GSH into vacuole-derived vesicles. The in vivo tests described above indicate that Bpt1p function partially overlaps that of Ycf1p. To compare Bpt1p- and Ycf1p-dependent transport biochemically, we isolated yeast vacuolar membranes from wild-type, single-mutant, and double-mutant strains and examined their capacities to mediate the MgATP-energized transport of three canonical MRP substrates: the GSH conjugate DNP-GS, the glucuronate conjugate $E_2$17βG, and reduced GSH. For all of these substrates, it was found that the transport capabilities of Bpt1p overlapped with those of Ycf1p to varying degrees; for two of the three substrates, Bpt1p appeared to require Ycf1p for maximal activity.

Vesicular DNP-GS uptake was the first transport function to be assayed, because this model GS conjugate is firmly established as a substrate for Ycf1p. When assayed for time dependence at a concentration of 10 μM, DNP-GS uptake by WT vesicles was 18.8 nmol of substrate in 5 min (Fig. 4A, inset). Uptake by vesicles from a *bpt1*Δ single mutant was 13.5 nmol of substrate in 5 min, representing a 28% decrease from the transport capacity of the WT and indicating a modest but observable contribution of Bpt1p to MgATP-dependent transport of this conjugate. By contrast, the amount of DNP-GS uptake by vesicles from a *ycf1*Δ single mutant and from a *ycf1*Δ *bpt1*Δ double mutant was <0.2 nmol of substrate in 5 min,

representing a >95% decrease in transport capacity compared to that of the WT.

These effects were similarly evident in the concentration dependence of DNP-GS uptake (Fig. 4A). In a WT strain, the bulk of the transport measured is attributable to Ycf1p, since vesicles from a *ycf1*Δ strain are markedly decreased in their transport efficacy compared to vesicles from a WT strain. The K_m for the WT versus *ycf1*Δ vesicles is 5.8 ± 2.3 versus 268.4 ± 157.0 μM; the corresponding V_{max} values are 30.7 ± 2.3 versus 20.3 ± 7.8 nmol/mg/10 min, respectively (Fig. 4A). In contrast to *YCF1*, the effects of disrupting the *BPT1* gene were modest: K_m was negligibly affected relative to that of the WT (6.3 ± 3.8 versus 5.8 ± 2.3 μM) and V_{max} was only slightly attenuated (25.3 ± 3.0 versus 30.7 ± 2.3 nmol/mg/10 min) (Fig. 4A). As expected if Ycf1p mediates the bulk of DNP-GS transport, the difference between the concentration-dependent uptake by *ycf1*Δ single-mutant membranes and that by *ycf1*Δ *bpt1*Δ double-mutant membranes was small (Fig. 4A).

By comparison with that of DNP-GS, transport of the other substrates, the glucuronate conjugate $E_2$17βG (Fig. 4B) and reduced GSH (Fig. 4C), followed a different pattern. In both cases, the relative contribution made by Bpt1p was greater, implying that that this transporter has a preference for $E_2$17βG and GSH over DNP-GS. Vesicles from the *bpt1*Δ strain show a 59% decrease in the capacity for uptake of 100 μM $E_2$17βG (1.8 nmol of substrate in 5 min versus a WT value of 4.4 nmol of substrate in 5 min) (Fig. 4B, inset). However, unexpectedly, the contributions of Bpt1p and Ycf1p are not additive, as a decrease in the amount of $E_2$17βG uptake in the *ycf1*Δ single mutant was >95%, not 41%. This low level of uptake was similar to that of the *ycf1*Δ *bpt1*Δ double mutant (Fig. 4B).

A pattern comparable to that seen for $E_2$17βG was also observed for GSH. Disruption of the *BPT1* gene diminished the total capacity of the membranes for transport by more than 40%, whereas uptake of GSH was negligible throughout the concentration range examined not only in the membrane vesicles from *ycf1*Δ *bpt1*Δ double-mutant cells but also in those from *ycf1*Δ single-mutant cells (Fig. 4C).

***BPT1* and *YCF1* are differentially regulated transcriptionally.** Yap1p is a transcription factor that modulates the expression of a large number of yeast genes implicated in the response to oxidative stress, for instance, stress resultant from exposure to cadmium (31, 50). Since *YCF1* is under the regulatory control of Yap1p, it was of interest to determine whether *BPT1* expression shares this characteristic. To compare the influence of Yap1p on the expression patterns of *YCF1* and *BPT1*, we generated constructs in which the 5′ upstream regions of *YCF1* and *BPT1* were fused to the coding region of *lacZ*. These reporter plasmids were transformed into WT, *yap1*-defective, or *YAP1*-overexpressing strains that were subsequently assayed for β-galactosidase activity (Table 4).

Two features are evident from these expression studies. First, the basal levels of *YCF1* and *BPT1* expression in a WT strain are essentially the same (Table 4, rows 1 and 6), suggesting that in the absence of inducer these transporters are present at similar levels. Second, while the expression of *YCF1* is strongly modulated by Yap1p, *BPT1* expression is only marginally affected if at all. Mutational loss of Yap1p activity results in an approximately 3-fold decrease in *YCF1* expression. Conversely, Yap1p overexpression leads to an approximately 10-fold increase in *YCF1* expression (Table 4, compare rows 2 and 3 to row 1). This is in complete agreement with the results of previous studies (50). In strict contrast, *BPT1* expression was not affected by a lack of Yap1p and was only modestly increased (~1.5-fold) by an excess of Yap1p.

TABLE 4. Comparison of the transcriptional regulation of *YCF1* and *BPT1*

Trial no.	Strain[a] or substrate concentration	β-Galactosidase activity[b] of strain bearing the indicated fusion construct	
		P_{YCF1}-*lacZ*	P_{BPT1}-*lacZ*
1	SEY6210 (WT)	2.53 ± 0.12	2.37 ± 0.12
2	SM13 (*yap1*Δ)	0.85 ± 0.07	2.17 ± 0.08
3	SM13 (*yap1*Δ YEp351-*YAP1*)	22.93 ± 0.85	3.26 ± 0.07
4	60 mg of adenine/liter	3.14 ± 0.15	2.22 ± 0.11
5	0 mg of adenine/liter	15.76 ± 0.7	5.40 ± 0.36
6	0 μM $CdCl_2$	2.72 ± 0.45	2.34 ± 0.34
7	50 μM $CdCl_2$	6.72 ± 0.84	3.70 ± 0.47

[a] Strain ABC154 (*ade2*) was used for each trial unless otherwise specified.
[b] Measured as described in Materials and Methods and expressed as β-galactosidase units per OD_{600} unit of cells.

Expression of the fusion constructs was also examined under conditions of adenine deficiency and excess in order to assess the effects of endogenous AIR-GS conjugates on *YCF1* and *BPT1* expression. Limiting levels of adenine (0 μg/ml) elicited an approximately 5-fold increase in P_{YCF1}-*lacZ* expression over that in cells subjected to excess adenine (60 μg/ml), but an increase of only 2.5-fold in P_{BPT1}-*lacZ* expression (Table 4, compare rows 5 and 4). Analogous experiments employing cadmium at 0 and 50 μM as an inducer increased the expression of P_{YCF1}-*lacZ* and P_{BPT1}-*lacZ* by approximately 2.5- and 1.5-fold, respectively (Table 4, compare rows 6 and 7). The strong induction of *YCF1* observed under conditions of high cadmium and limiting adenine may be partly or wholly mediated through Yap1p. The modest transcriptional effects seen for Bpt1p may also be mediated by Yap1p, or instead by another, as yet undetermined transcription factor.

DISCUSSION

Bpt1p and Ycf1p are localized to the vacuolar membrane and show overlapping transport properties in vivo. In this study we compared the localization, expression, and substrate transport properties of Bpt1p and its close homologue Ycf1p in order to gain more insight into the MRP subfamily of ABC transporters in yeast. The sequence and structural similarities between Bpt1p and Ycf1p suggest that they might have similar functions in vivo. To initiate studies of Bpt1p, we compared the localization of C-terminally GFP-tagged Ycf1p and Bpt1p in vivo. Fluorescence microscopy revealed that the localization of Bpt1p-GFP is indeed vacuolar, like that of Ycf1p-GFP (Fig. 1). These findings corroborate and extend the results of previous in vitro experiments showing that vacuole-enriched membrane preparations, which are at best only partially pure, mediate Bpt1p-dependent transport activity (34, 37).

The vacuolar localization of Bpt1p is consistent with the notion that it, like Ycf1p, contributes to the vacuolar sequestration of otherwise toxic compounds. Several possibilities can be envisioned for how these transporters might function in the

same intracellular environment. For example, Bpt1p and Ycf1p could have identical substrate transport and regulatory properties, and so function redundantly. Alternatively, these transporters could have a distinct pattern of substrate selectivity and regulation, and function complementarily. Finally, a combination of both of these schemes could apply, such that Bpt1p and Ycf1p might exhibit functional and regulatory overlap under some circumstances and unique properties under others. As detailed below, the latter combined view seems to best explain the properties of Bpt1p and Ycf1p both in vivo and in vitro.

To directly compare the contributions of Bpt1p and Ycf1p in vivo, we generated *bpt1*Δ and *ycf1*Δ (single) and *ycf1*Δ *bpt1*Δ (double) mutants. Neither *YCF1* nor *BPT1* is essential for viability. We used these mutants to examine two well-characterized phenotypes known to involve Ycf1p: *ade2* pigmentation and cadmium resistance. These substrates were considered to be particularly appropriate because they share the property of being conjugated to, or complexed with, GSH yet are either of endogenous (the biosynthetic intermediate AIR) or exogenous (cadmium) origin. We show here that Bpt1p, like Ycf1p, plays a role in *ade2* pigmentation and cadmium detoxification (Table 3; Fig. 2 and 3). While Ycf1p accounted for most of the transport measured for both substrates, Bpt1p made a minor but demonstrable contribution. Specifically, in the *ycf1*Δ single mutant, *ade2* pigmentation was strongly reduced (by 70%) compared to that in the WT, and growth in the presence of Cd^{2+} was strongly inhibited (by 64% at 100 μM $CdCl_2$) (Table 3). Although the *bpt1*Δ mutation alone did not result in a defect in *ade2* pigmentation or cadmium resistance, a function for Bpt1p was clearly evident in the *ycf1*Δ *bpt1*Δ double mutant, whose phenotype was significantly more severe than that of the *ycf1*Δ single mutant. Both *ade2* pigment accumulation and growth in 100 μM $CdCl_2$ (Table 3) were reduced by a further 15% in the *ycf1*Δ *bpt1*Δ double mutant versus the *ycf1*Δ single mutant.

The phenomenon observed here for Bpt1p, in which the single *bpt1*Δ and *ycf1*Δ mutants show no phenotype, or only a modest one, but the double mutant is severely impaired, can be referred to as "synthetic enhancement" (15). Generally, genes which exhibit synthetic enhancement are intimately connected functionally, either as interacting components or, in the case of deletion mutations, more likely as functionally redundant proteins. With Bpt1p and Ycf1p, the latter mode of synthetic enhancement is the more likely. Thus, Ycf1p alone (i.e., in a *bpt1*Δ mutant) is sufficient for full transport of the substrates tested in vivo here. In the absence of Ycf1p (i.e., in a *ycf1*Δ mutant), there is still residual function. This must be due to Bpt1p, since in the *ycf1*Δ *bpt1*Δ double mutant, transport is decreased even further. Independent corroboration of the ability of Bpt1p to function as a transporter is provided by the finding that its overexpression in the *ycf1*Δ *bpt1*Δ double mutant rescues the *ade2* pigmentation defect (Fig. 2).

***BPT1* and *YCF1* are differentially regulated.** The smaller contribution of Bpt1p, compared to Ycf1p, to the transport of in vivo substrates could be due solely to the distinct substrate preferences of these transporters. Alternatively, or additionally, the lower contribution of Bpt1p could reflect a lower relative level of expression than that of Ycf1p. The possibility of differentially regulated expression of *YCF1* versus *BPT1* is supported by promoter fusion studies (Table 4). *YCF1* expression is exquisitely sensitive to the dosage of Yap1p, a transcription factor involved in responses to oxidative stress. P_{YCF1}-*lacZ* expression is decreased 3-fold in the absence of Yap1p and is increased 10-fold when Yap1p is overexpressed. In contrast, P_{BPT1}-*lacZ* expression exhibits no, or at most very little, dependence on Yap1p; it is insensitive to the absence of Yap1p and only modestly elevated (~1.5-fold) by Yap1p overexpression. Since cadmium resistance involves regulatory effects exerted through Yap1p, it is not surprising that P_{YCF1}-*lacZ* expression is increased to a greater extent than that of P_{BPT1}-*lacZ* in 50 μM Cd (~2.5- versus 1.5-fold, respectively [Table 4]). It is established that the strong Cd^{2+}-induced increase in *YCF1* expression is indeed dependent on Yap1p (50), but it is not known if the modest increase in *BPT1* expression elicited by Cd^{2+} is mediated by Yap1p or by another transcription factor.

By analogy with the results obtained with Cd^{2+}, we find that P_{YCF1}-*lacZ* expression is substantially induced (fivefold) under conditions of adenine limitation, in which the *ade2* pigment precursor (AIR) is present, while *BPT1* expression is only modestly induced (twofold). Thus, the presence of the *ade2* pigment precursor results in overrepresentation of Ycf1p relative to Bpt1p. It is instructive to note that it is the presence of substrate and not the growth conditions per se that result in *YCF1* induction, since in a WT *ADE2* strain exposed to conditions of adenine limitation, this induction does not occur (K. G. Sharma and A. K. Bachhawat, unpublished data).

Extrapolating from our gene expression data in Table 4, it is likely that at the level of protein expression Ycf1p and Bpt1p are roughly equivalent under normal conditions. However, the relative amounts of Ycf1p may exceed those of Bpt1p when cells are treated with Cd^{2+}. Therefore, Ycf1p should make proportionately the greatest contribution to Cd^{2+} resistance in WT cells, masking the contribution of Bpt1p. Thus, differences in *BPT1* and *YCF1* gene expression mediated through Yap1p and potentially other transcription factors may be largely responsible for the distinct phenotypic contributions of Bpt1p and Ycf1p in vivo. Clearly, the ability of these transporters to be differentially regulated expands the range of environmental or endogenous insults which yeast cells can tolerate.

Bpt1p and Ycf1p exhibit distinct substrate preferences in in vitro transport assays. We were interested in comparing the transport properties of Bpt1p and Ycf1p for canonical MRP substrates in vitro. To do so, we isolated a vacuolar membrane-enriched fraction from WT, single-mutant, and double-mutant cells and determined the kinetics of transport of a model GS conjugate (DNP-GS), a model glucuronate conjugate ($E_2$17βG), and unconjugated GSH. The activity we measured in the in vitro transport assay (Fig. 4) reflects the basal levels of Bpt1p and Ycf1p, since the cells used for preparation of the vacuole-enriched fraction were grown in the absence of inducer. From the results of these in vitro measurements, it is clear that Bpt1p and Ycf1p overlap in their transport capabilities but exhibit distinct substrate preference profiles. On the one hand, Bpt1p appears to favor glucuronate conjugates and free GSH over GS conjugates (Fig. 4). On the other hand, vesicles from a *ycf1*Δ mutant are severely (>95%) impaired for the transport of all three substrates, suggesting that Ycf1p plays a major and essential role in the transport of all three substrates (see below).

Although for the substrates tested here, *ycf1*Δ vesicles were less effective in transport than *bpt1*Δ vesicles, this pattern ap-

pears not to be universal for all substrates. Two recent studies examined the substrate transport properties for unconjugated bile pigment (UCB) (37) and several MRI contrast reagents (Gd-EOB·DTPA, Gd-BOPTA, Gd-B 20790, and Gd-B 21690) (34), comparing vesicles from WT and mutant strains. Taken together, the results from our study and those previous studies show that Ycf1p is the major (>50%) contributor to the transport of UCB, Gd-BOPTA, DNP-GS, $E_2$17βG, and GSH. In contrast, Bpt1p and Ycf1p contribute approximately equally to Gd-B 20790 transport, and Bpt1p is the major contributor to Gd-EOB·DPTA transport. This pattern of overlapping but nonidentical substrate preference for yeast MRPs is reminiscent of what has been documented for the mammalian MRP1 to MRP5 proteins (20, 22) and the vacuolar GS conjugate pumps AtMRP1 and AtMRP2 from plants (26–28), suggesting that this is a recurrent theme within the MRP subfamily in all organisms.

A notable difference between the in vitro transport of some substrates (i.e., $E_2$17βG [this study]) and that of others (i.e., UCB) (37) is the lack of additivity of Bpt1p and Ycf1p activities. For example, since we observed a 59% diminution of $E_2$17βG transport in *bpt1*Δ vacuolar membrane vesicles, we expected that the equivalent fraction from *ycf1*Δ cells would show a reduction of ≤41%. However, unexpectedly, what we saw instead was a diminution of >95% in the *ycf1*Δ single-mutant strain and no further reduction of transport activity in the *ycf1*Δ *bpt1*Δ double-mutant strain. Thus, Bpt1p appears to contribute to the transport of $E_2$17βG (Fig. 4B), and similarly GSH (Fig. 4C), only in the presence of Ycf1p. How might this surprising dependence be explained? One model to account for these findings is that Bpt1p and Ycf1p may interact combinatorially to form a heterodimer. For the three substrates tested here, such a Bpt1p/Ycf1p heterodimer would have optimal transport activity, while Bpt1p alone or as a homodimer is inactive and Ycf1p alone or as a homodimer has intermediate activity. This model is appealing not only because it is consistent with the present data but also in light of a recent structural study of MRP1 which suggests that it exists predominantly as a dimeric structure (39). An alternative model is that another component which is lacking or down-regulated in both the *ycf1*Δ and *ycf1*Δ *bpt1*Δ strains is necessary for maximal Bpt1p activity.

MRP proteins in yeast. Comparison of the yeast MRP proteins Bpt1p and Ycf1p highlights the point that despite their sequence similarity, MRPs can exhibit biologically important differences, including differential substrate specificity and regulatory properties. There are four additional genes that encode MRPs in yeast: *YBT1* (first published as *BAT1*), *YOR1*, *YHL035*, and *YKR103*/*YKR104* (12, 45). Sequence alignments suggest that all of these contain a full or partial N-terminal extension. Ybt1p is a vacuolar membrane protein that can transport bile acid, but apparently not GS-conjugated compounds (33), and Yor1p is a plasma membrane protein that plays a role in oligomycin resistance (13, 19). The products of the remaining two genes, *YHL035* and *YKR103*/*YKR104*, remain uncharacterized. It is noteworthy that the latter actually encodes two adjacent reading frames separated by a nonsense codon, likely representing a sequencing error or a mutation in the strain used to sequence the yeast genome. It is clear from the present study that developing a complete picture of detoxification and related processes in yeast will require an understanding of the distinct localization patterns, expression profiles, and substrate transport properties of all of the yeast MRPs.

ACKNOWLEDGMENTS

We thank Scott Moye-Rowley for the *YAP1* strains and plasmids.

A.K.B. was supported by a grant from the Department of Science and Technology, Government of India. K.G.S. was a recipient of a Senior Research Fellowship from the Council of Scientific and Industrial Research of India. S.M. was supported by grants GM51508 and DK58029 from the National Institutes of Health. P.A.R. was supported by grants NRICGP 99-35304-8094 and DE-FG02-91ER20055 from the U.S. Department of Agriculture and U.S. Department of Energy, respectively.

K. G. Sharma and D. L. Mason contributed equally to this work.

REFERENCES

1. **Ambudkar, S. V., S. Dey, C. A. Hrycyna, M. Ramachandra, I. Pastan, and M. M. Gottesman.** 1999. Biochemical, cellular, and pharmacological aspects of the multidrug transporter. Annu. Rev. Pharmacol. Toxicol. **39:**361–398.
2. **Borst, P., R. Evers, M. Kool, and J. Wijnholds.** 2000. A family of drug transporters: the multidrug resistance-associated proteins. J. Natl. Cancer Inst. **92:**1295–1302.
3. **Borst, P., R. Evers, M. Kool, and J. Wijnholds.** 1999. The multidrug resistance protein family. Biochim. Biophys. Acta **1461:**347–357.
4. **Brachmann, C. B., A. Davies, G. J. Cost, E. Caputo, J. Li, P. Hieter, and J. D. Boeke.** 1998. Designer deletion strains derived from *Saccharomyces cerevisiae* S288C: a useful set of strains and plasmids for PCR-mediated gene disruption and other applications. Yeast **14:**115–132.
5. **Chaudhuri, B., S. Ingavale, and A. K. Bachhawat.** 1997. *apd1*+, a gene required for red pigment formation in *ade6* mutants of *Schizosaccharomyces pombe*, encodes an enzyme required for glutathione biosynthesis: a role for glutathione and a glutathione-conjugate pump. Genetics **145:**75–83.
6. **Chen, P., S. Sapperstein, J. D. Choi, and S. Michaelis.** 1997. Biogenesis of the *Saccharomyces cerevisiae* mating pheromone **a**-factor. J. Cell Biol. **136:** 251–269.
7. **Cole, S. P., and R. G. Deeley.** 1998. Multidrug resistance mediated by the ATP-binding cassette transporter protein MRP. Bioessays **20:**931–940.
8. **Coleman, S. T., E. Tseng, and W. S. Moye-Rowley.** 1997. *Saccharomyces cerevisiae* basic region-leucine zipper protein regulatory networks converge at the *ATR1* structural gene. J. Biol. Chem. **272:**23224–23230.
9. **Costanzo, M. C., M. E. Crawford, J. E. Hirschman, J. E. Kranz, P. Olsen, L. S. Robertson, M. S. Skrzypek, B. R. Braun, K. L. Hopkins, P. Kondu, C. Lengieza, J. E. Lew-Smith, M. Tillberg, and J. I. Garrels.** 2001. YPD, PombePD and WormPD: model organism volumes of the BioKnowledge library, an integrated resource for protein information. Nucleic Acids Res. **29:**75–79.
10. **Dean, M., Y. Hamon, and G. Chimini.** 2001. The human ATP-binding cassette (ABC) transporter superfamily. J. Lipid Res. **42:**1007–1017.
11. **Dean, M., A. Rzhetsky, and R. Allikmets.** 2001. The human ATP-binding cassette (ABC) transporter superfamily. Genome Res. **11:**1156–1166.
12. **Decottignies, A., and A. Goffeau.** 1997. Complete inventory of the yeast ABC proteins. Nat. Genet. **15:**137–145.
13. **Decottignies, A., A. M. Grant, J. W. Nichols, H. de Wet, D. B. McIntosh, and A. Goffeau.** 1998. ATPase and multidrug transport activities of the overexpressed yeast ABC protein Yor1p. J. Biol. Chem. **273:**12612–12622.
14. **Ghosh, M., J. Shen, and B. P. Rosen.** 1999. Pathways of As(III) detoxification in *Saccharomyces cerevisiae*. Proc. Natl. Acad. Sci. USA **96:**5001–5006.
15. **Guarente, L.** 1993. Synthetic enhancement in gene interaction: a genetic tool come of age. Trends Genet. **9:**362–366.
16. **Guarente, L., and M. Ptashne.** 1981. Fusion of *Escherichia coli lacZ* to the cytochrome *c* gene of *Saccharomyces cerevisiae*. Proc. Natl. Acad. Sci. USA **78:**2199–2203.
17. **Higgins, C. F.** 1992. ABC transporters: from microorganisms to man. Annu. Rev. Cell Biol. **8:**67–113.
18. **Hipfner, D. R., R. G. Deeley, and S. P. Cole.** 1999. Structural, mechanistic and clinical aspects of MRP1. Biochim. Biophys. Acta **1461:**359–376.
19. **Katzmann, D., T. Hallstrom, M. Voet, W. Wysock, J. Golin, G. X. Volckaert, and W. Moye-Rowley.** 1995. Expression of an ATP-binding cassette transporter-encoding gene (*YOR1*) is required for oligomycin resistance in *Saccharomyces cerevisiae*. Mol. Cell. Biol. **15:**6875–6883.
20. **Keppler, D., T. Kamisako, I. Leier, Y. Cui, A. T. Nies, H. Tsujii, and J. Konig.** 2000. Localization, substrate specificity, and drug resistance conferred by conjugate export pumps of the MRP family. Adv. Enzyme Regul. **40:**339–349.
21. **Konig, J., A. T. Nies, Y. Cui, I. Leier, and D. Keppler.** 1999. Conjugate export pumps of the multidrug resistance protein (MRP) family: localization, sub-

strate specificity, and MRP2-mediated drug resistance. Biochim. Biophys. Acta **1461:**377–394.
22. **Kruh, G., H. Zeng, P. Rea, G. Liu, K. Lee, and M. Belinsky.** 2001. MRP subfamily transporters and resistance to anticancer agents. J. Bioenerg. Biomembr. **33:**493–501.
23. **Li, Z., M. Szczypka, Y. Lu, D. Thiele, and P. Rea.** 1996. The yeast cadmium factor protein (YCF1) is a vacuolar glutathione S-conjugate pump. J. Biol. Chem. **271:**6509–6517.
24. **Li, Z., Y. Zhao, and P. Rea.** 1995. Magnesium adenosine 5′-triphosphate-energized transport of glutathione S-conjugates by plant vacuolar membrane vesicles. Plant Physiol. **107:**1257–1268.
25. **Li, Z. S., Y. P. Lu, R. G. Zhen, M. Szczypka, D. J. Thiele, and P. A. Rea.** 1997. A new pathway for vacuolar cadmium sequestration in *Saccharomyces cerevisiae*: YCF1-catalyzed transport of bis(glutathionato)cadmium. Proc. Natl. Acad. Sci. USA **94:**42–47.
26. **Liu, G., R. Sanchez-Fernandez, Z. S. Li, and P. A. Rea.** 2001. Enhanced multispecificity of *Arabidopsis* vacuolar multidrug resistance-associated protein-type ATP-binding cassette transporter, AtMRP2. J. Biol. Chem. **276:** 8648–8656.
27. **Lu, Y. P., Z. S. Li, Y. M. Drozdowicz, S. Hortensteiner, E. Martinoia, and P. A. Rea.** 1998. AtMRP2, an *Arabidopsis* ATP binding cassette transporter able to transport glutathione S-conjugates and chlorophyll catabolites: functional comparisons with Atmrp1. Plant Cell **10:**267–282.
28. **Lu, Y. P., Z. S. Li, and P. A. Rea.** 1997. *AtMRP1* gene of *Arabidopsis* encodes a glutathione S-conjugate pump: isolation and functional definition of a plant ATP-binding cassette transporter gene. Proc. Natl. Acad. Sci. USA **94:**8243–8248.
29. **Marquardt, D.** 1963. An algorithm for nonlinear estimation of nonlinear parameters. J. Soc. Ind. Appl. Math. **11:**431–441.
30. **Michaelis, S., and I. Herskowitz.** 1988. The **a**-factor pheromone of *Saccharomyces cerevisiae* is essential for mating. Mol. Cell. Biol. **8:**1309–1318.
31. **Moye-Rowley, W. S., K. D. Harshman, and C. S. Parker.** 1989. Yeast *YAP1* encodes a novel form of the Jun family of transcriptional activator proteins. Genes Dev. **3:**283–292.
32. **Oldenburg, K. R., K. T. Vo, S. Michaelis, and C. Paddon.** 1997. Recombination-mediated PCR-directed plasmid construction *in vivo* in yeast. Nucleic Acids Res. **25:**451–452.
33. **Ortiz, D. F., M. V. St. Pierre, A. Abdulmessih, and I. M. Arias.** 1997. A yeast ATP-binding cassette-type protein mediating ATP-dependent bile acid transport. J. Biol. Chem. **272:**15358–15365.
34. **Pascolo, L., S. Petrovic, F. Cupelli, C. V. Bruschi, P. L. Anelli, V. Lorusso, M. Visigalli, F. Uggeri, and C. Tiribelli.** 2001. ABC protein transport of MRI contrast agents in canalicular rat liver plasma vesicles and yeast vacuoles. Biochem. Biophys. Res. Commun. **282:**60–66.
35. **Paulusma, C. C., M. Kool, P. J. Bosma, G. L. Scheffer, F. ter Borg, R. J. Scheper, G. N. Tytgat, P. Borst, F. Baas, and R. P. Oude Elferink.** 1997. A mutation in the human canalicular multispecific organic anion transporter gene causes the Dubin-Johnson syndrome. Hepatology **25:**1539–1542.
36. **Paulusma, C. C., and R. P. Oude Elferink.** 1997. The canalicular multispecific organic anion transporter and conjugated hyperbilirubinemia in rat and man. J. Mol. Med. **75:**420–428.
37. **Petrovic, S., L. Pascolo, R. Gallo, F. Cupelli, J. D. Ostrow, A. Goffeau, C. Tiribelli, and C. V. Bruschi.** 2000. The products of *YCF1* and YLL015w (*BPT1*) cooperate for the ATP-dependent vacuolar transport of unconjugated bilirubin in *Saccharomyces cerevisiae*. Yeast **16:**561–571.
38. **Rose, M. D., F. Winston, and P. Hieter.** 1990. Methods in yeast genetics. A laboratory course manual. Cold Spring Harbor Press, Cold Spring Harbor, N.Y.
39. **Rosenberg, M. F., Q. Mao, A. Holzenburg, R. C. Ford, R. G. Deeley, and S. P. Cole.** 2001. The structure of the multidrug resistance protein 1 (MRP1/ABCC1). Crystallization and single-particle analysis. J. Biol. Chem. **276:** 16076–16082.
40. **Sanchez-Fernandez, R., T. G. Davies, J. O. Coleman, and P. A. Rea.** 2001. The *Arabidopsis thaliana* ABC protein superfamily, a complete inventory. J. Biol. Chem. **276:**30231–30244.
41. **Sharma, K. G., V. Sharma, A. Bourbouloux, S. Delrot, and A. K. Bachhawat.** 2000. Glutathione depletion leads to delayed growth stasis in *Saccharomyces cerevisiae*: evidence of a partially overlapping role for thioredoxin. Curr. Genet. **38:**71–77.
42. **Sikorski, R. S., and P. Hieter.** 1989. A system of shuttle vectors and yeast host strains designed for efficient manipulation of DNA in *Saccharomyces cerevisiae*. Genetics **122:**19–27.
43. **Siliciano, P., and K. Tatchell.** 1984. Transcription and regulatory signals at the mating type locus in yeast. Cell **37:**969–978.
44. **Szczypka, M. S., J. A. Wemmie, W. S. Moye-Rowley, and D. J. Thiele.** 1994. A yeast metal resistance protein similar to human cystic fibrosis transmembrane conductance regulator (CFTR) and multidrug resistance-associated protein. J. Biol. Chem. **269:**22853–22857.
45. **Taglicht, D., and S. Michaelis.** 1998. *Saccharomyces cerevisiae* ABC proteins and their relevance to human health and disease. Methods Enzymol. **292:** 130–162.
46. **Tommasini, R., R. Evers, E. Vogt, C. Mornet, G. Zaman, A. Schinkel, P. Borst, and E. Martinoia.** 1996. The human multidrug resistance-associated protein functionally complements the yeast cadmium resistance factor 1. Proc. Natl. Acad. Sci. USA **93:**6743–6748.
47. **Wach, A., A. Brachat, R. Pohlmann, and P. Philippsen.** 1994. New heterologous modules for classical or PCR-based gene disruptions in *Saccharomyces cerevisiae*. Yeast **10:**1793–1808.
48. **Wada, M., S. Toh, K. Taniguchi, T. Nakamura, T. Uchiumi, K. Kohno, I. Yoshida, A. Kimura, S. Sakisaka, Y. Adachi, and M. Kuwano.** 1998. Mutations in the canilicular multispecific organic anion transporter (cMOAT) gene, a novel ABC transporter, in patients with hyperbilirubinemia II/Dubin-Johnson syndrome. Hum. Mol. Genet. **7:**203–207.
49. **Wemmie, J., and W. Moye-Rowley.** 1997. Mutational analysis of the *Saccharomyces cerevisiae* ATP-binding cassette transporter protein Ycf1p. Mol. Microbiol. **25:**683–694.
50. **Wemmie, J., M. Szczypka, D. Thiele, and W. Moye-Rowley.** 1994. Cadmium tolerance mediated by the yeast AP-1 protein requires the presence of an ATP-binding cassette transporter-encoding gene, *YCF1*. J. Biol. Chem. **269:** 32592–32597.